Distribution and isotopic compositions of *n*-alkanes and *n*-alkenes in the cryoconites from the Tibetan Plateau glaciers

Quanlian Li[1,2] , Shichang Kang[1,3], Shijin Wang[1,2], Ninglian Wang[4,5,6], Xiaobo Wu[1], Wasim Sajjad[1], Huan Yang[7], Yao Li[1] and Jingquan Wu[1]

[1]Northwest Institute of Eco-Environment and Resources, State Key Laboratory of Frozen Soil Engineering, SKLCS Lanzhou, Gansu, CN, CAS, Lanzhou 730000, China; [2]Yulong Snow Mountain Station of Cryosphere and Sustainable Development, State Key Laboratory of Cryospheric Sciences, Northwest Institute of Eco-Environment and Resources, Chinese Academy of Sciences, Lanzhou 730000, China; [3]University of Chinese Academy of Sciences, Beijing 100049, China; [4]Shaanxi Key Laboratory of Earth Surface System and Environmental Carrying Capacity, Xi'an 710127, China; [5]Institute of Earth Surface System and Hazards, Northwest University, Xi'an 710127, China; [6]College of Urban and Environmental Sciences, Northwest University, Xi'an 710127, China and [7]Hubei Key Laboratory of Critical Zone Evolution, School of Geography and Information Engineering, China University of Geosciences, Wuhan 430074, China

Abstract

In the current study, cryoconite samples were collected from six glaciers on the Tibetan Plateau to analyze *n*-alkanes and *n*-alkenes. The findings revealed that the concentrations of *n*-alkanes and *n*-alkenes varied from 40.1 to 496.1 $\mu g\,g^{-1}$ and from 4.6 to 13.8 $\mu g\,g^{-1}$, respectively. The carbon preference index of the long-chain *n*-alkanes ranged from 3.3 to 8.4, and the average chain length ranged from 28.7 to 29.3. Moreover, the $\delta^{13}C$ of the *n*-alkanes in cryoconites were within the range of C_3 plants, demonstrating that the *n*-alkanes in cryoconites were only derived from vascular plants. However, the δD_{mean} were more negative than that of C_3 plants, which could be caused by dry and humid conditions of glaciers. Unlike *n*-alkanes, *n*-alkenes ranged from $C_{17:1}$ to $C_{30:1}$ and showed a weak even-over-odd carbon number preference in the Dongkemadi, Yuzhufeng, Laohugou and Tianshan glacier, but a weak odd carbon preference in the Qiyi glacier. The *n*-alkenes in the YL Snow Mountains showed an obvious odd-over-even carbon number predominance from $C_{17:1}$ to $C_{22:1}$ with C_{max} at $C_{19:1}$, and the even-over-odd carbon number preference from $C_{23:1}$ to $C_{30:1}$ with C_{max} at $C_{28:1}$. This demonstrated that the *n*-alkenes of cryoconites may be mainly derived from *in situ* production in glaciers.

1. Introduction

Cryoconites are dark-colored, spherical granules on the glacier surface (Langford and others, 2014; Cook and others, 2016; Takeuchi and others, 2018). Cryoconite granules are often composed of filamentous cyanobacteria entangled with minerals and organic particles (Takeuchi and others, 2014). Due to their darker tone, cryoconites can absorb more solar radiation than the surrounding ice, which promote the melting of the ice beneath the granules and form cryoconite holes (Chandler and others, 2015; Tedesco and others, 2016). Cryoconite holes are regarded as unique glacier ecosystems, in which liquid water is available on the glacier surface during the ablation season. Therefore, cryoconite holes could act as biologically active habitats for a diverse community of microorganisms, including algae, cyanobacteria, bacteria, archaea, viruses, rotifers, tardigrades and insects (Bagshaw and others, 2016; Zhou and others, 2019; Rozwalak and others, 2022). Generally, algae and cyanobacteria usually grow at the bottom of cryoconite holes, and they produce organic matter through photosynthesis, which supports the proliferation of heterotrophs (Takeuchi and others, 2018).

The organic matter accumulated on cryoconites usually has both autochthonous and allochthonous sources (Hood and others, 2009; Singer and others, 2012; Stibal and others, 2012). The autochthonous organic matter in cryoconites is produced *in situ* via heterotrophic or autotrophic microbial activities (Anesio and others, 2009; Smith and others, 2017), whereas allochthonous organic matter (such as levoglucosan) may be derived from biomass burning (Li and others, 2019). However, the particles deposited on glaciers as well as the autochthonous and allochthonous organic matter are darker, so they reduce the albedo of the glacier surface and accelerate glacier melting (Takeuchi and others, 2001; Takeuchi, 2002; Rozwalak and others, 2022). Until now, there have been only sporadic reports on organic matters in cryoconites. Xu and others (2010) found normal alkanes in cryoconites from Athabasca Glacier of Mount Rocky, Canada were derived from mossy and vascular plant origin. They also detected higher concentrations of phospholipid fatty acid, indicating that the glacier surface was dominated by Gram-positive and Gram-negative bacteria, as well as cyanobacteria. Pautler and others (2013) also found that Antarctic cryoconites contained microbial proteins, peptides and phospholipid fatty acids. The above results suggested these organic matters in cryoconites from Arctic and Antarctic were derived from the combined contributions of both higher plants and *in situ* microorganism's activities.

Normal alkanes (*n*-alkanes), which are stable, long-lived and non-polar-saturated hydrocarbon molecules that originate from epicuticular waxes of vascular higher plants (Eglinton and Hamilton, 1967; Bush and McInerney, 2013; Diefendorf and Freimuth, 2017). Short-chain *n*-alkanes in the range of C_{14}–C_{22} are produced mainly by bacteria, algae and microbial organisms (Han and Calvin, 1969; Grimalt and Albaiges, 1987). Mid-chain *n*-alkanes (C_{23}–C_{25}) have been mainly detected in aquatic macrophytes (Ficken and others, 2000). *n*-Alkanes are strongly recalcitrant due to their hydrophobic nature and excellent chemical stability during transportation, deposition and burial (Schwark and others, 2002). Moreover, the stable carbon isotope compositions ($\delta^{13}C$) of *n*-alkanes in different matrixes have been widely employed to understand their source regions because they are sensitive to the plant types (C_3 or C_4) they are derived from (Chikaraishi and Naraoka, 2003; Schefuß and others, 2005; Hockun and others, 2016). In addition, the hydrogen isotope ratios (δD) of higher plant waxes, primarily reflect the δD of the precipitation during photosynthesis (Sachse and others, 2006, 2012). Hence, the combination of distribution and dual-isotope ratios ($\delta^{13}C$ and δD) of *n*-alkanes provides a powerful tool for accessing their source regions (Diefendorf and Freimuth, 2017; Zhang and others, 2023). Compared with the *n*-alkanes, the *n*-alkenes are geologically unstable due to the sensitivity of the double bond to oxidation. The long-chain *n*-alkanes and *n*-alkenes have been detected previously in Antarctic soils (Matsumoto and others, 1990), peat (Xie and others, 2004) and sediments (Zhang and others, 2015; Pu and others, 2017). However, investigations for these compounds in the glacier are still a fairly novel field. Therefore, to fill this information gap, the cryoconite samples were collected from six glaciers on the Tibetan Plateau (TP) to probe the molecular distribution characteristics of *n*-alkanes and *n*-alkenes in cryoconites and discussed their potential sources based on $\delta^{13}C$ and δD. For the first time, this paper provides an account of the unusual distribution of *n*-alkenes in cryoconites from the TP and discusses their possible origins.

2. Materials and methods

2.1. Study site

During July and August 2014, cryoconite samples were collected from six glaciers which are presented in Figure 1 and the

Table 1. Information about the cryoconite samples collected from different glaciers on the Tibetan Plateau

	Glacier	Latitude	Longitude	Altitude range m a.s.l.	Sample number
Southeastern TP	YL Snow Mountains	27°40′ N	100°11′ E	4637–4825	9
Central TP	DKMD	33°35′ N	92°43′ E	5464–5657	6
	YZF	35°39′ N	94°14′ E	5226–5454	3
Northern TP	QY	39°14′ N	97°46′ E	4356–4766	11
	LHG	39°28′ N	96°33′ E	4386–4850	13
	TS	43°06′ N	86°48′ E	3772–4000	14

sampling information is provided in Table 1. The Ürümqi Tianshan (TS) Glacier No.1 is located on the eastern side of the Tien Shan (Fig. 1). The Laohugou (LHG) Glacier No. 12 and the Qiyi (QY) glacier are located on the northern slope of the Qilian Mountains in the northeastern TP. The Yuzhufeng (YZF) glacier is located on the eastern Kunlun Mountains in the northern TP. These four glaciers are affected by the westerlies throughout the year. The Dongkemadi (DKMD) glacier is located on the northern slope of the Tanggula Mountains in the central TP, which is the transitional region of the South Asian monsoon and westerly winds. The Baishui Glacier No. 1 (YL Snow Mountains) is located in the southeastern TP, which has a typical Indian monsoon climate.

2.2. Sample collection

The cryoconite samples were collected from the ablation areas of each glacier using a sterile stainless-steel scoop. All samples were sealed and labeled immediately and stored in a freezer at −20°C until further analysis.

2.3. Extraction and measurement

The cryoconite samples were lyophilized at −70°C and ground into powder. Cryoconite powder (20 g) was extracted using a Soxhlet extractor with dichloromethane and methanol (9:1 v/v) for 72 h. The aliphatic hydrocarbon fractions were loaded onto precleaned silica gel columns and were eluted with hexane. The aliphatic hydrocarbons fractions were determined by a gas
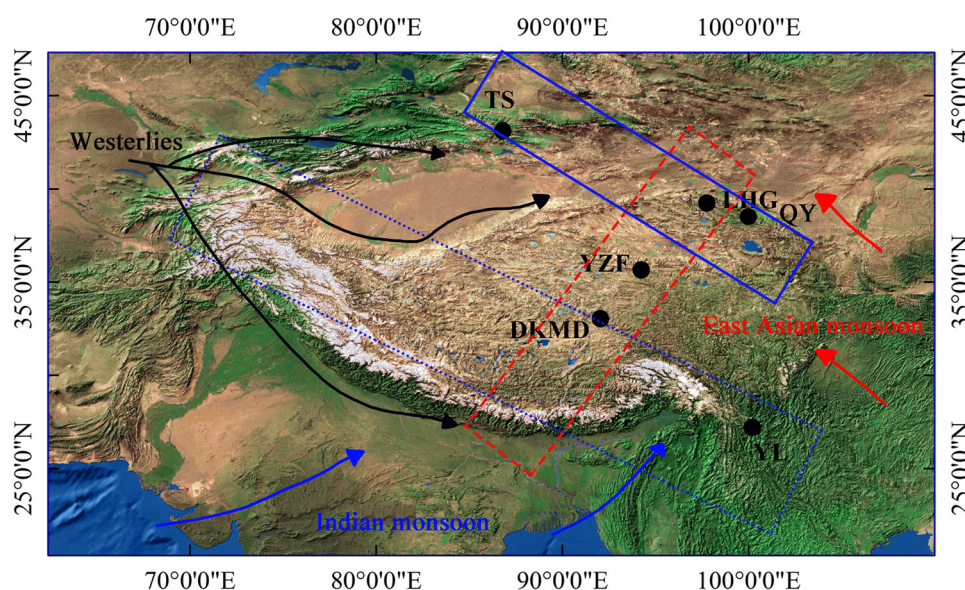

Figure 1. Sampling sites of cryoconites on the TP glaciers.

chromatography–mass spectrometry (GC–MS) using an Agilent 7890A gas chromatograph coupled with an Agilent 5975C mass spectrometer. The chromatographic column was a DB-1 MS capillary column (30 m × 0.25 mm × 0.25 μm). The GC oven temperature was programmed from 70 to 320°C in steps of 4°C min⁻¹ and held for 30 min. Samples were injected in splitless mode (1 μL) and high purity helium (99.999%) was used as the carrier gas at a flow rate of 1.0 mL min⁻¹. The ion source temperature was 250°C, and ionization energy was 70 eV. The full scanning mode was used to select the characteristic ions (m/z 85) for the detection of n-alkanes. The identification and quantification of n-alkanes were achieved by comparing peak areas with external n-alkane standards (mixture of C_{21}, C_{25}, C_{27}, C_{29}, C_{31} and C_{33}) of known concentration.

Compound-specific carbon and hydrogen isotopes were measured using an HP 6890 GC, interfaced with a Finnigan MAT Delta plus XL isotope ratio mass spectrometry instrument by a high temperature pyrolysis reactor. In all analyses, an Agilent HP-1 MS (30 m × 0.32 mm i.d., 0.25 μm film thickness) capillary column was used, and helium was used as the carrier gas. δ¹³C and δD values are reported in per mil (‰) relative to Vienna Pee Dee Belemnite and Vienna Standard Mean Ocean Water, respectively. Each sample was independently measured thrice. Isotopic measurements were calibrated by coinjected 4–6 n-alkane standards. Detailed experimental procedure of compound-specific carbon and hydrogen isotope can be found in Bi and others (2005). Achieved precision, expressed as the average std dev., was 4‰ for the standard mixtures.

2.4. n-Alkane indices

The carbon preference index (CPI) and the average chain length (ACL) were used as n-alkane indices. The CPI measures the odd-over-even carbon number predominance of the n-alkane, which is used to characterize the sources of n-alkane (Eglinton and Hamilton, 1967). The ACL of n-alkanes from the higher plant is predominantly a function of vegetation type (Li and others, 2013). The CPI and ACL were calculated as follows:

$$CPI_{n\text{-alkanes}} =$$
$$\frac{1}{2} \times \left[\frac{\sum_{odd}(C_{25} - C_{33})}{\sum_{even}(C_{24} - C_{32})} + \frac{\sum_{odd}(C_{25} - C_{33})}{\sum_{even}(C_{26} - C_{34})} \right] \quad (1)$$

$$ACL_{n\text{-alkanes}} =$$
$$\frac{27 \times C_{27} + 29 \times C_{29} + 31 \times C_{31} + 33 \times C_{33} + 35 \times C_{35}}{C_{27} + C_{29} + C_{31} + C_{33} + C_{35}} \quad (2)$$

$$CPI_{18:1-24:1} =$$
$$\frac{1}{2} \times \left[\frac{\sum_{odd}(C_{19:1} - C_{23:1})}{\sum_{even}(C_{18:1} - C_{22:1})} + \frac{\sum_{odd}(C_{19:1} - C_{23:1})}{\sum_{even}(C_{20:1} - C_{24:1})} \right] \quad (3)$$

$$CPI_{23:1-30:1} =$$
$$\frac{1}{2} \times \left[\frac{\sum_{odd}(C_{23:1} - C_{29:1})}{\sum_{even}(C_{22:1} - C_{28:1})} + \frac{\sum_{odd}(C_{23:1} - C_{29:1})}{\sum_{even}(C_{24:1} - C_{30:1})} \right] \quad (4)$$

Odd-over-even predominance (OEP), similar to CPI, is another n-alkane ratio proxy for the predominance of odd-over-even. The OEP of n-alkanes and n-alkenes were calculated as follows:

$$OEP_{n\text{-alkanes}} = \frac{C_{27} + C_{29} + C_{31}}{C_{26} + C_{28} + C_{30}} \quad (5)$$

$$OEP_{17:1-22:1} = \frac{C_{17:1} + C_{19:1} + C_{21:1}}{C_{18:1} + C_{20:1} + C_{22:1}} \quad (6)$$

$$OEP_{23:1-30:1} = \frac{C_{23:1} + C_{25:1} + C_{27:1} + C_{29:1}}{C_{24:1} + C_{26:1} + C_{28:1} + C_{30:1}} \quad (7)$$

3. Results and discussion

3.1. Concentrations of the aliphatic hydrocarbons in cryoconites

The concentrations of the n-alkanes and n-alkenes in cryoconite samples of different glaciers varied from 36.5 to 496.1 μg g⁻¹ and from 4.8 to 17.0 μg g⁻¹, respectively (Fig. 2). The average concentration of n-alkanes was highest in the YL Snow Mountains (496.1 ± 68.0 μg g⁻¹) and the lowest in the DKMD Glacier (36.5 ± 3.9 μg g⁻¹). The average concentrations of n-alkanes were 118.9 ± 5.7 μg g⁻¹ in the TS Glacier, 76.0 ± 2.7 μg g⁻¹ in the LHG Glacier, 70.2 ± 8.2 μg g⁻¹ in the QY Glacier, and 49.8 ± 6.4 μg g⁻¹ in the YZF Glacier. Similarly, the highest total concentration of n-alkenes was measured in the YL Snow Mountains (17.0 ± 5.0 μg g⁻¹), while the lowest concentration was measured in the YZF Glacier (4.8 ± 2.1 μg g⁻¹) rather than in the DKMD Glacier (7.2 ± 0.7 μg g⁻¹). Overall, n-alkanes are 4.6–29.3 times larger than the corresponding carbon number of n-alkenes in six glaciers. Moreover, the concentrations of n-alkane in the cryoconites were much higher than those previously reported in Antarctic soil (0.013–2.2 μg g⁻¹ from n-C_{14} to n-C_{35}) (Matsumoto and others, 1990), but lower than those in the cryoconites reported in Western Canada (290–2990 μg g⁻¹ from n-C_{18} to n-C_{33}) (Pautler and others, 2013) and other Antarctic soil (800–13 400 μg g⁻¹ from n-C_{18} to n-C_{33}) (Xu and others, 2010).

3.2. Distribution characteristics of n-alkanes

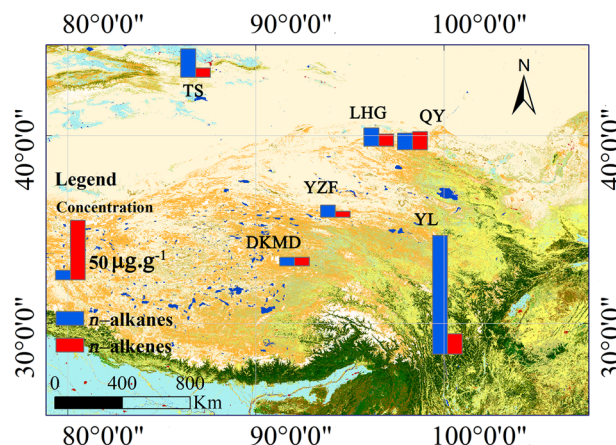Vascular plants typically show a strong odd-over-even carbon number predominant distribution, with a maximum abundance

Figure 2. Concentration of n-alkanes and n-alkenes in cryoconites.

at n-C_{27}, n-C_{29} or n-C_{31} (Eglinton and Hamilton, 1967; Collister and others, 1994). The CPI values of n-alkanes from higher plants are generally >5 (Eglinton and Hamilton, 1967), whereas the n-alkanes from lower organisms, such as bacteria and algae, as well as fossil fuels, have low CPI values close to 1 (El Nemr and others, 2016). The average relative abundance of the n-alkanes and n-alkenes in the cryoconites of different glaciers is shown in Figure 3. The cryoconite samples in the DKMD, YZF, QY, LHG and TS glaciers contain a suite of n-alkanes ranging from n-C_{14} to n-C_{35}, with C_{max} values at n-C_{29} or n-C_{31}. This finding is comparable with the distribution of n-alkanes in 154 lacustrine surface sediments on the TP (Xia and others, 2008). The n-alkanes in the YL Snow Mountains show the wider distribution

ranged from n-C_{13} to n-C_{37} compared with the other five glaciers. However, the n-alkanes of n-C_{18}, n-C_{19} and n-C_{20} in the DKMD, YZF, QY, LHG and TS glaciers and n-C_{19} in the YL Snow Mountains are below detection limit. The GC–MS figure is provided in Supplementary information 1.

As shown in Table 2, the average CPI values of the n-C_{25} to n-C_{33} n-alkanes in the cryoconites varied from 3.3 in the YL Snow Mountains to 8.4 in the QY Glacier (Table 2), similar to the Japan Sea sediments (Yamada and Ishiwatari, 1999), showing an obvious odd-over-even carbon number predominance, which indicates that the n-alkanes in cryoconites were derived from higher plants. The CPI value is the lowest in the YL Snow Mountains, because the higher CPI values usually correlate with
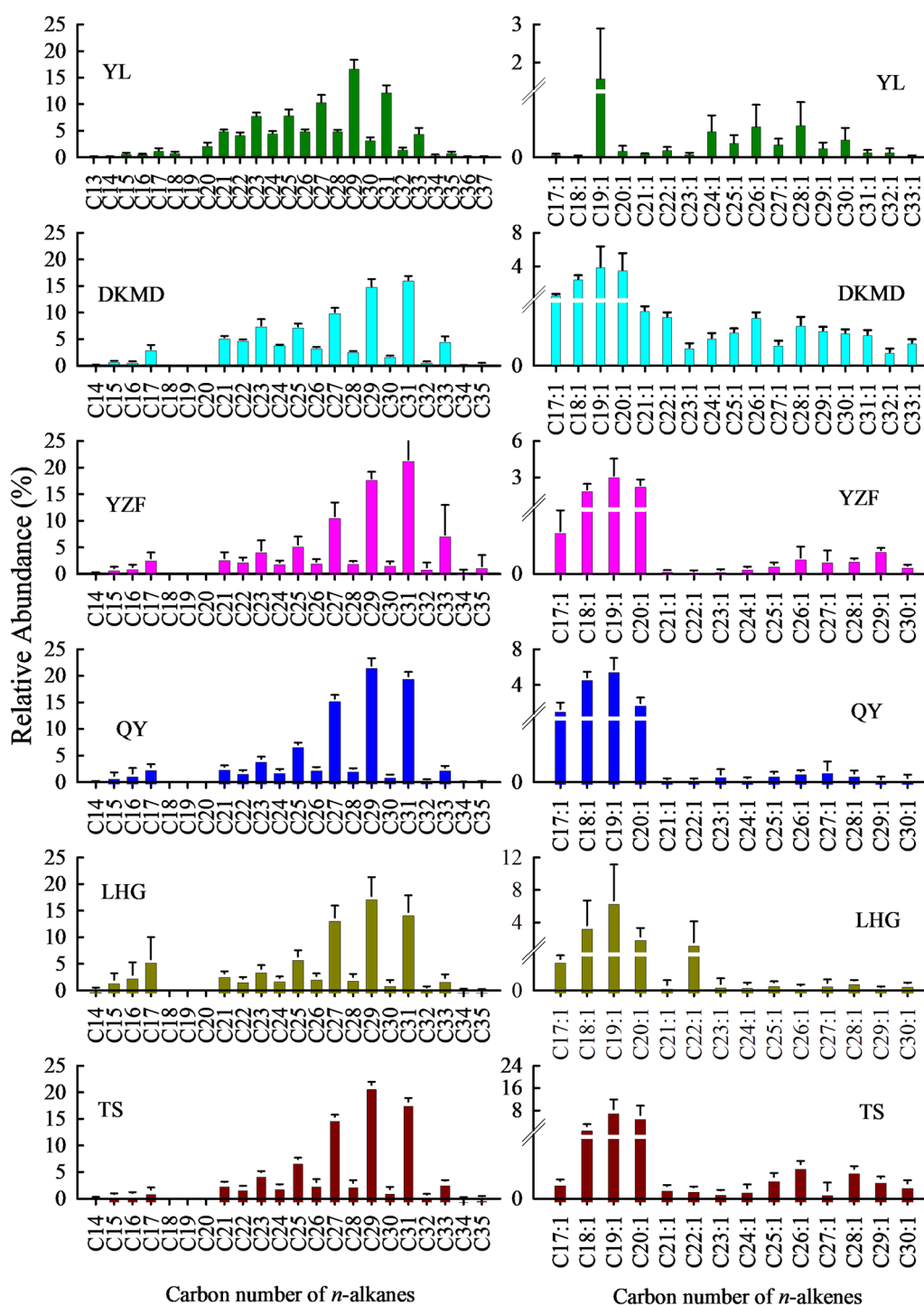

Figure 3. Average relative abundances of the n-alkanes and n-alkenes in the cryoconites.

Table 2. Molecular distribution of the *n*-alkanes and *n*-alkenes in the cryoconites

	Sample	YL	DKMD	YZF	QY	LHG	TS
n-alkanes	CPI_{25-33}	3.3 ± 0.4	5.2 ± 0.1	7.5 ± 0.6	8.4 ± 0.7	6.5 ± 1.3	6.9 ± 1.3
	OEP	2.7	5.2	7.7	8.6	7.2	5.2
	ACL	28.8 ± 0.2	29.0 ± 0.2	29.1 ± 0.1	28.9 ± 0.1	28.7 ± 0.1	28.8 ± 0.1
	C_{27}/C_{31}	0.82	0.50	0.66	0.71	0.82	0.89
	L/H[a]	0.13	0.11	0.11	0.09	0.16	0.09
n-alkenes	$CPI_{17:1-22:1}$	4.40	0.89	1.02	1.87	1.35	1.15
	$OEP_{17:1-22:1}$	6.32	0.76	0.82	1.03	0.98	0.98
	$CPI_{23:1-30:1}$	0.39	0.69	0.96	1.15	0.56	0.66
	$OEP_{23:1-30:1}$	0.37	0.72	0.89	1.12	0.91	0.65
	L/H[b]	0.69	11.19	9.03	23.40	5.56	17.56

"a" indicated the $\Sigma C_{21}^-/\Sigma C_{22}^+$ of *n*-alkanes, "b" indicated the $\Sigma C_{21}^-/\Sigma C_{22}^+$ of *n*-alkenes.

cold and dry environments, whereas the smaller CPI values usually correlate with warm and humid environments (Ankit and others, 2017). In addition, CPI values were also related to local vegetation type (Bai and others, 2019). The OEP value of *n*-alkanes in the polluted substrates is in the range of 1.0–1.2 (Snedaker and others, 1995), so OEP can determine whether the sedimentary area is polluted by petroleum hydrocarbons (Snedaker and others, 1995). The OEP of cryoconites ranged from 2.7 to 8.6, indicating that cryoconites on the TP glaciers were not polluted by petroleum and its derivatives. However, previous studies showed that unpolluted environments had stable ACL values (Sikes and others, 1993). The ACL of >27 represents an input of terrigenous higher plants (Ankit and others, 2017). In these six glaciers, the ACL of the cryoconite sample varied from 28.8 to 29.3, it was basically stable at ∼29, indicating that the main source of *n*-alkanes in cryoconites was terrestrial higher plants.

For *n*-alkanes, the *n*-C_{27} and *n*-C_{29} are diagnostic of woody plants while the *n*-C_{31} is diagnostic of herbaceous plants (Meyers, 2003). Therefore, the *n*-C_{27}/*n*-C_{31} ratio of *n*-alkanes is usually used to evaluate the relative contribution of herbaceous and woody plants (Meyers, 2003; Bush and McInerney, 2013). The ratio of *n*-C_{27}/*n*-C_{31} < 1 indicates an input increase of herbaceous plants, and the ratio of *n*-C_{27}/*n*-C_{31} > 1 indicates an input increase of woody plants. The ratio of *n*-C_{27}/*n*-C_{31} in cryoconites ranged from 0.50 and 0.89, which indicates *n*-alkanes in TP glaciers could be mainly derived from herbaceous plants. The $\Sigma C_{21}^-/\Sigma C_{22}^+$ ratio of *n*-alkanes reflect the relative abundance changes of lower bacterial algae organisms and higher plants (Meyers, 2003). When $\Sigma C_{21}^-/\Sigma C_{22}^+$ < 1, it indicates that the soils are in the early development stage and greatly influenced by the input of terrigenous higher plants. The $\Sigma C_{21}^-/\Sigma C_{22}^+$ of *n*-alkanes is between 0.09 and 0.16, indicating that *n*-alkanes in cryoconites mainly come from terrigenous higher plants, and cryoconite has not been formed in soil.

3.3. Distributions and source of n-*alkenes*

The *n*-alkenes ranged from $C_{17:1}$ to $C_{30:1}$ with a C_{max} value of *n*-$C_{19:1}$ and were detected in all cryoconite samples (Fig. 3). The relatively *n*-alkene abundance of $C_{17:1}-C_{20:1}$ in DKMD, YZF, QY, LHG, and TS glaciers were higher than that of $C_{21:1}-C_{30:1}$. Moreover, *n*-alkenes with $C_{17:1}-C_{30:1}$ were also detected in lower concentration than the corresponding *n*-alkanes. The *n*-alkenes in the YL Snow Mountains showed a bimodal distribution ranging from $C_{17:1}$ to $C_{33:1}$. The main peak was $C_{19:1}$ and the second peak was $C_{28:1}$, which was in line with the occurrence of the *n*-alkenes in lake sediments (Pu and others, 2017) and Antarctic soils (Matsumoto and others, 1990). The $CPI_{17:1-23:1}$ and $OEP_{17:1-22:1}$ of *n*-alkenes were 4.40 and 6.32, respectively. Meanwhile, the $CPI_{23:1-30:1}$ and

$OEP_{23:1-30:1}$ of *n*-alkenes were 0.39 and 0.37 in the YL Snow Mountains, respectively. This demonstrated an obvious odd-over-even carbon number predominance from $C_{17:1}$ to $C_{22:1}$, and an even-over-odd carbon number preference from $C_{23:1}$ to $C_{30:1}$ in the YL Snow Mountains. The $CPI_{17:1-23:1}$ and $OEP_{17:1-22:1}$ of *n*-alkenes in the DKMD, YZF, LHG and TS glaciers ranged from 0.89 to 1.35 and from 0.76 to 0.98, respectively. The $CPI_{23:1-30:1}$ and $OEP_{23:1-30:1}$ of *n*-alkenes in the DKMD, YZF, LHG and TS glaciers ranged from 0.56 to 0.96 and from 0.65 to 0.91, respectively. This showed a weak even-over-odd carbon number preference from $C_{17:1}$ to $C_{30:1}$ in these four glaciers. In contrast, the $CPI_{17:1-23:1}$ and $OEP_{17:1-22:1}$ of *n*-alkenes in the QY Glacier were 1.87 and 1.03, respectively. The $CPI_{23:1-30:1}$ and $OEP_{23:1-30:1}$ of *n*-alkenes in the QY Glacier were 1.15 and 1.12, respectively. This showed a weak odd-over-even carbon number predominance from $C_{17:1}$ to $C_{30:1}$ in the QY Glacier. The $\Sigma C_{21}^-/\Sigma C_{22}^+$ of *n*-alkenes were 0.69 in the YL Snow Mountains, and ranged from 5.56 to 23.40 in the other five glaciers, demonstrating that *n*-alkenes in the YL Snow Mountains has a different source from the other five glaciers.

The *n*-alkenes coexisted with *n*-alkanes in the cryoconite, but it was inferred that *n*-alkene has a different source from *n*-alkane due to the unusual distribution characteristic, different carbon number ranges and C_{max} between them. Previous studies indicated that *n*-alkenes could originate from rare cases, e.g. the epicuticular waxes of higher plants (Grimalt and Albaigés, 1990; Pu and others, 2018), algae, fungi and cyanobacteria organisms living in aquatic environment (Patterson, 1967; Gelpi and others, 1968, 1970; Matsumoto and others, 1990), the reduction of diagenesis of monounsaturated fatty acids for the main source of *n*-alkene (Ekpo and others, 2005) and the microbial transformation of the corresponding *n*-alkanes or direct inputs from organisms (Jaffé and others, 2001). The relatively *n*-alkene abundance of $C_{17:1}-C_{20:1}$ in the DKMD, YZF, QY, LHG and TS glaciers was higher than that of $C_{21:1}-C_{30:1}$, and the *n*-alkanes of C_{18}, C_{19} and C_{20} were below detection limit. This indicated that $C_{17:1}$, $C_{18:1}$, $C_{19:1}$ and $C_{20:1}$ *n*-alkenes in the DKMD, YZF, QY, LHG and TS glaciers could be derived from the microbial transformation of the corresponding *n*-alkanes. However, *n*-alkenes were not detected in aerosols and the surface soil around the TP glacier (Matsumoto and others, 1990; Bai and others, 2014), which combined with the special distribution in the cryoconites determines that the *n*-alkenes in the cryoconites are from microorganisms.

Cryoconite holes are covered by ice lids and snow accumulation on the glacier, which can keep them isolated from the atmosphere. Therefore, wind-borne materials cannot be deposited in cryoconite holes in winter (Foreman and others, 2007). During the summer melting season, as the snow and ice on the glacier slowly melt, more and more cryoconite holes are opened to the atmosphere, and more microbes enter or *in situ* production occurs in the cryoconite holes (Musilova and others, 2017).

According to the previous reports (Takeuchi and others, 2001), a large amount of snow algae is contained in the cryoconite. Singer and others (2012) identified a prominent population of unsaturated aliphatic lipids and peptides in glaciers, which supports the *in situ* production of these compounds by microorganisms. Antony and others (2014) reported that the aliphatic molecules (double bond equivalents per carbon atom) were most likely produced from microbial and algal biomass, constituting ∼37–52% of the total formulas assigned to each glacial ice sample. Moreover, a large number of cyanobacteria have been identified on glacial surfaces on the TP (Takeuchi and Li, 2008; Liu and others, 2009; Feng and others, 2016). Therefore, we conclude that *n*-alkene identified in the cryoconites from the TP glacier may have been mainly produced *in situ* by various microbes. More knowledge is needed about the biosynthetic origins of long-chain *n*-alkenes and factors deciding their accumulation in cryoconites.

3.4. Carbon stable isotope compositions of n-*alkanes*

Figure 4 illustrates the $\delta^{13}C$ values of the *n*-alkanes (*n*-C_{27}, *n*-C_{29}, *n*-C_{31}) in the cryoconite samples of six glaciers. Generally, the $\delta^{13}C$ values of the *n*-C_{29} and *n*-C_{31} alkanes in most glaciers were more negative than those of the *n*-C_{27} alkanes. The difference was likely due to the involvement of different biosynthetic pathways of these long-chain *n*-alkanes (Collister and others, 1994). In this study, the $\delta^{13}C$ values of the *n*-C_{29} and *n*-C_{31} *n*-alkanes were more negative in the YL Snow Mountains than those of the other five glaciers. The reason may be that YL Snow Mountains are located in the southeastern TP and are a part of the southern Hengduan Mountains, which have a warm, humid climate and surrounded by dense vegetation. In contrast, cold and dry climate highly influence the other five glaciers, because the compound-specific carbon isotopic values of the long-chain *n*-alkanes are sensitive to regional moisture (Wiltshire and others, 2023). A previous study indicated that ^{13}C enrichment in plants occurs under drought stress because leaf stomata are closed to prevent transpiration. Therefore, the ratio of intercellular to the ambient CO_2 concentration decreases, resulting in increased carbon isotope fractionation (Diefendorf and Freimuth, 2017). DKMD and YZF glaciers in the central TP are surrounded by Taklamakan Desert and the Qaidam Basin with sparse vegetation coverage and arid climate. In summer, the evaporation of the soil water and leaf surface water is stronger in the central TP than in the YL Snow Mountains and QY, LHG and TS glaciers. Therefore, the largest $\delta^{13}C$ values of the *n*-C_{27}, *n*-C_{29} and *n*-C_{31} *n*-alkanes ranged from −32.0 to

−31.4‰ in the YZF Glacier and from −33.5 to −31.7‰ in the DKMD Glacier. The TS, QY and LHG glaciers are all located in the northern edge of the TP, which has a lower relative humidity than the southeastern TP. The $\delta^{13}C$ values of the *n*-C_{27}, *n*-C_{29} and *n*-C_{31} *n*-alkanes detected in the northern edge of TP were at intermediate levels, ranging from −33.7 to −32.9‰ in the TS Glacier, from −33.3 to −30.8‰ in the QY Glacier and from −34.5 to −31.9‰ in the LHG Glacier. Similar *n*-alkane distributions have been documented in the snow pits from the TP glacier (Xie and others, 2000; Li and others, 2009), fresh snow in Sapporo, northern Japan (Yamamoto and others, 2011) and fresh snow in Hokkaido, Japan (Sankelo and others, 2013).

The $\delta^{13}C$ of *n*-alkanes can provide information on the source of organic materials (Aichner and others, 2010a). For example, plants with different photosynthetic pathways have distinctive $\delta^{13}C$ values: C_3 plants produce long-chain *n*-alkanes with $\delta^{13}C$ values between −32 and −39‰, while C_4 plants have $\delta^{13}C$ values between −18 and −25‰ (Collister and others, 1994). A quantitative estimate of the relative contribution of C_3 plants, compared to that of C_4 plants, was conducted using the $\delta^{13}C$ of the *n*-alkanes and a binary mixing model. The isotopic composition and relative abundance of *n*-C_{27}, *n*-C_{29}, and *n*-C_{31} alkanes in each cryoconite sample were used to calculate their weighted mean $\delta^{13}C$ values ($\delta^{13}C_{mean}$) (Eqn (8)). According to a previous study, the end-member values for wax *n*-alkanes should be −36‰ for C_3 plants and −21‰ for C_4 plants (Collister and others, 1994). In Eqn (8), C_n is the concentration (units). The relative contribution of C_3 plants (*f*) was calculated using Eqn (9). The hydrogen isotope compositions and relative abundances of the *n*-C_{27}, *n*-C_{29} and *n*-C_{31} alkanes in each cryoconite sample were used to calculate their weighted mean δD values (δD_{mean}) (Eqn (10)):

$$\delta^{13}C_{mean} = \frac{\delta^{13}C_{27} \times C_{27} + \delta^{13}C_{29} \times C_{29} + \delta^{13}C_{31} \times C_{31}}{C_{27} + C_{29} + C_{31}} \quad (8)$$

$$\delta^{13}C_{mean} = f(-36‰) + (1-f)(-21‰) \quad (9)$$

$$\delta D_{mean} = \frac{D_{27} \times C_{27} + D_{29} \times C_{29} + D_{31} \times C_{31}}{C_{27} + C_{29} + C_{31}} \quad (10)$$

As shown in Table 3, the weighted mean $\delta^{13}C$ values ($\delta^{13}C_{mean}$) of the *n*-C_{27}, *n*-C_{29} and *n*-C_{31} *n*-alkanes in all cryoconite samples ranged from −31.7 to −34.8‰. The $\delta^{13}C_{mean}$ values were −34.8‰ ± 1.4 in the YL Snow Mountains, −32.9‰ ± 1.3 in the DKMD Glacier, −31.7‰ ± 0.3 in the YZF Glacier, −32.2‰ ± 1.3 in the QY Glacier, −33.7‰ ± 1.4 in the LHG Glacier and −33.2 ± 0.5‰ in the TS Glacier. The application of the two end-member mixing models revealed that C_3 plants contributed 71.3–92.2% of the total *n*-alkanes in the cryoconites from all glaciers (Table 3), indicating that C_3 plants were the dominant source of the *n*-alkanes in the cryoconites on the TP glaciers.

3.5. Hydrogen stable isotope compositions of n-*alkanes*

In all cryoconites, the δD values of the predominant odd carbon number of *n*-alkanes could be measured, but that of the even carbon number of *n*-alkanes could not be measured due to their low abundance. The measured δD values of the odd carbon number of *n*-alkanes (*n*-C_{27}, *n*-C_{29} and *n*-C_{31}) and weighted mean δD values ($\delta D_{mean‰}$) of the *n*-C_{27}, *n*-C_{29} and *n*-C_{31} are listed in Table 3. Previous studies indicated that the δD_{wax} value of woody, shrub and herbaceous plants decreased sequentially (Hou and others, 2007). In this study, the C_{max} value was *n*-C_{31} in the cryoconite
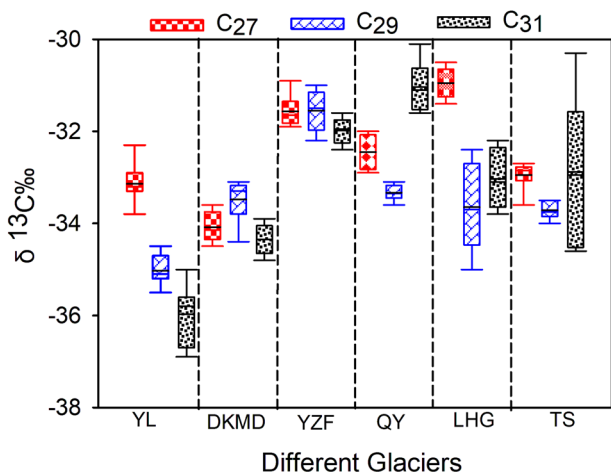

Figure 4. Box plots of the mean $\delta^{13}C$ values of the *n*-alkanes in all six glaciers.

Table 3. δD and δ¹³C values of individual *n*-alkanes in cryoconites

	YL Snow Mountains	DKMD	YZF	QY	LHG	TS
n-Alkane (δ¹³C)						
$\delta^{13}C_{27}$ (‰)	−34.2	−33.1	−31.7	−32.5	−31.9	−33.0
$\delta^{13}C_{29}$ (‰)	−35.0	−33.5	−31.4	−33.3	−34.5	−33.7
$\delta^{13}C_{31}$ (‰)	−36.0	−31.7	−32.0	−30.8	−34.3	−32.9
$\delta^{13}C_{mean}$ (‰)[a]	−34.8 ± 1.4	−32.9 ± 1.3	−31.7 ± 0.3	−32.2 ± 1.3	−33.7 ± 1.4	−33.2 ± 0.5
C_3 (%)	92.0	79.0	71.3	74.3	84.5	81.5
C_4 (%)	7.8	21.0	28.7	25.7	15.5	18.5
n-Alkane (δD)						
C_{27} (‰)	−191.6	−202.2	−163.7	−162.9	−153.0	−171.8
C_{29} (‰)	−181.0	−198.4	−172.5	−168.5	−159.2	−174.8
C_{31} (‰)	−181.9	−209.3	−179.7	−178.0	−171.0	−207.0
δD_{mean} (‰)[b]	−183.5 ± 7.2	−203.5 ± 9.1	−174 ± 6.1	−170.7 ± 6.3	−158.7 ± 6.8	−178.1 ± 13.6

[a]Abundance weighted mean δ¹³C value ($\delta^{13}C_{mean‰}$) of the *n*-C₂₇, *n*-C₂₉ and *n*-C₃₁ *n*-alkanes.
[b]Abundance weighted mean δD values ($\delta D_{mean‰}$) of the *n*-C₂₇, *n*-C₂₉ and *n*-C₃₁ *n*-alkanes.

of the DKMD and YZF glaciers, which was consistent with the vegetation coverage around the DKMD and YZF glaciers, indicating that the terrestrial *n*-alkanes in the cryoconite of these two glaciers mainly came from herbaceous plants around the glaciers. Therefore, the δD$_{mean}$ of the DKMD Glacier was the most negative (−203.5 ± 9.1) among the six glaciers. However, the YZF Glacier is located near the Qaidam Basin with cold and dry climate, so the δD$_{mean}$ value of the YZF Glacier was relatively more positive (−174 ± 6.1) than the DKMD Glacier. In the cryoconites of the other four glaciers, including YL Snow Mountains and QY, LHG and TS glaciers, the C_{max} was *n*-C₂₉ in these four glaciers, which mainly came from woody plants and shrubs. The vegetation and precipitation of YL Snow Mountains was more abundant than that of the other five glaciers. As a result, the δD$_{mean}$ value of YL Snow Mountains was the only second negative (−183.5 ± 7.2) to the DKMD Glacier. The δD$_{mean}$ values from DKMD and YL Snow Mountains were more negative than that from the other four glaciers, consistent with the local river and water vapor isotopic characteristics (Li and Garzioner, 2017). The TS, QY and LHG glaciers all belong to cold and dry climate, but the air temperature and precipitation in the TS Glacier were higher than those in the QY and LHG glaciers. However, the woody plants, shrubs and vegetation in the TS Glacier were more abundant than in the QY and LHG glaciers. Therefore, the δD$_{mean}$ value of TS Glacier (−178.1 ± 13.6) was more negative than that of QY Glacier (−170.7 ± 6.3) and LHG Glacier (−162.7 ± 6.8).

The plot of δ¹³C versus δD of six glaciers is presented in Figure 5. The weighted mean δ¹³C values of the *n*-C₂₇, *n*-C₂₉

and *n*-C₃₁ alkanes ranged from −33.3 to −35.0‰ in all the cryoconite samples, which were within the range of C_3 leaf wax (−30 to −37.9‰) (Bi and others, 2005). Moreover, the δ¹³C$_{mean}$ values of the *n*-alkanes in the cryoconites were consistent with the snow in Hokkaido (−28.2 to −34.4‰) (Sankelo and others, 2013) and lake sediment on the TP (−20.3 to −35.8‰) (Aichner and others, 2010a). The weighted mean δD values of the *n*-C₂₇, *n*-C₂₉ and *n*-C₃₁ alkanes ranged from −153.0 to −212.3‰ in the cryoconites from the TP glaciers, which were within the range of the δD values of the *n*-alkane in snow from Hokkaido (−169.9 to −223.1‰) (Sankelo and others, 2013), lake sediments on the TP (−158.0 to −237‰) (Aichner and others, 2010b), and soil on the TP (−142.3 to −277.1‰) (Luo and others, 2011; Bai and others, 2014). However, these δD$_{mean}$ values were more negative than those of C_3 plant leaf wax (−95.9 to −209.1‰) (Bi and others, 2005), which could be potentially caused by glacial environment and the local climate due to low temperatures.

4. Conclusions

This study provides valuable information about the distribution and sources of *n*-alkanes and *n*-alkenes in the cryoconite samples of six glaciers on the TP. The *n*-alkanes ranged from *n*-C₁₄ to *n*-C₃₅, with a C_{max} value at *n*-C₂₉ or *n*-C₃₁ in the DKMD, YZF, QY, LHG and TS glaciers, but showed the wider distribution ranging from *n*-C₁₃ to *n*-C₃₇ in the YL Snow Mountains. The CPI is higher in the DKMD, YZF, QY, LHG and TS glaciers under cold and dry environments and the lowest in the YL Snow Mountains due to the higher environmental air temperature and precipitation. The ratio of *n*-C₂₇/*n*-C₃₁ ranged from 0.50 and 0.89, which indicates *n*-alkanes in TP glacier were mainly derived from herbaceous plants. The δ¹³C and δD values of the *n*-alkanes demonstrated that the isotopic signature of *n*-alkanes in cryoconites correlated with that derived only from vascular plants. The *n*-alkenes may have been mainly produced *in situ* by various microbes in the cryoconite due to their special distribution characteristics. The molecular distribution of the *n*-alkanes and *n*-alkenes in the cryoconites revealed that both allochthonous and autochthonous materials were essential contributors to the organic matters in the cryoconites on the TP glaciers.

Figure 5. Comparison of the average δ¹³C and δD values of the *n*-alkanes in all six glaciers.

References

Aichner B, Herzschuh U and Wilkes H (2010a) Influence of aquatic macrophytes on the stable carbon isotopic signatures of sedimentary organic matter in lakes on the Tibetan Plateau. *Organic Geochemistry* **41**(7), 706–718. doi: 10.1016/j.orggeochem.2010.02.002

Aichner B, Herzschuh U and Wilkes H (2010b) δD values of *n*-alkanes in Tibetan lake sediments and aquatic macrophytes – a surface sediment study and application to a 16 ka record from Lake Koucha. *Organic Geochemistry* **41**, 779–790. doi: 10.1016/j.orggeochem.2010.05.010

Anesio AM, Hodson AJ and Fritz A (2009) High microbial activity on glaciers: importance to the global carbon cycle. *Global Change Biology* **15**, 955–960. doi: 10.1111/j.1365-2486.2008.01758.x

Ankit Y, Mishra PK and Kumar P (2017) Molecular distribution and carbon isotope of *n*-alkanes from Ashtamudi Estuary, South India: assessment of organic matter sources and paleoclimatic implicatios. *Marine Chemistry* **196**(20), 62–70. doi: 10.1016/j.marchem.2017.08.002

Antony R, Grannas AM and Willoughby AS (2014) Origin and sources of dissolved organic matter in snow on the East Antarctic ice sheet. *Environmental Science Technology* **48**(11), 6151–6159. doi: 10.1021/es405246a

Bagshaw EA, Tranter M and Wadham JL (2016) Processes controlling carbon cycling in Antarctic glacier surface ecosystems. *Geochemical Perspectives Letters* **2**, 44–54. doi: 10.7185/geochemlet.1605

Bai Y, Tian Q and Fang XM (2014) The 'inverse altitude effect' of leaf wax-derived *n*-alkane δD on the northeastern Tibetan Plateau. *Organic Geochemistry* **73**, 90–100. doi: 10.1016/j.orggeochem.2014.05.013

Bai Y, Azamdzhon M and Wang S (2019) An evaluation of biological and climatic effects on plant *n*-alkane distributions and δ^2H_{alk} in a field experiment conducted in central Tibet. *Organic Geochemistry* **135**, 53–63. doi: 10.1016/j.orggeochem.2019.06.003

Bi XH, Sheng GY and Liu XH (2005) Molecular and carbon and hydrogen isotopic composition of *n*-alkanes in plant leaf waxes. *Organic Geochemistry* **36**(10), 1405–1417. doi: 10.1016/j.orggeochem.2005.06.001

Bush RT and McInerney FA (2013) Leaf wax *n*-alkane distributions in and across modern plants: implications for paleoecology and chemotaxonomy. *Geochimica et Cosmochimica Acta* **117**, 161–179. doi: 10.1016/J.GCA.2013.04.016

Chandler DM, Alcock JD and Wadham JL (2015) Seasonal changes of ice surface characteristics and productivity in the ablation zone of the Greenland Ice Sheet. *The Cryosphere* **9**(2), 487–504. doi: 10.5194/tcd-8-1337-2014

Chikaraishi Y and Naraoka H (2003) Compound-specific δD–δ13C analyses of *n*-alkanes extracted from terrestrial and aquatic plants. *Phytochemistry* **63**(3), 361–371. doi: 10.1016/S0031-9422(02)00749-5

Collister JW, Rieley G and Stern B (1994) Compound-specific δ13C of leaf lipids from plants with differing carbon dioxide metabolisms. *Organic Geochemistry* **21**(6/7), 619–627. doi: 10.1016/0146-6380(94)90008-6

Cook J, Edwards A and Takeuchi N (2016) Cryoconite: the dark biological secret of the cryosphere. *Progress in Physical Geography Earth and Environment* **40**(1), 66–111. doi: 10.1177/0309133315616574

Diefendorf AF and Freimuth EJ (2017) Extracting the most from terrestrial plant-derived *n*-alkyl lipids and their carbon isotopes from the sedimentary record: a review. *Organic Geochemistry* **103**, 1–21. doi: 10.1016/j.orggeochem.2016.10.016

Eglinton G and Hamilton RG (1967) Leaf epicuticular waxes. *Science* **156** (3780), 1322–1335. doi: 10.1126/science.156.3780.132

Ekpo BO, Oyo-Ita OE and Wehner H (2005) Even-*n*-alkane/alkene predominances in surface sediments from the Calabar River, SE Niger Delta, Nigeria. *Naturwissenschaften* **92**, 341–346. doi: 10.1007/s00114-005-0639-8

El Nemr A, Moneer AA and Ragab S (2016) Distribution and sources of *n*-alkanes and polycyclic aromatic hydrocarbons in shellfish of the Egyptian Red Sea coast. *The Egyptian Journal of Aquatic Research* **42**(2), 121–131. doi: 10.1016/j.ejar.2016.05.003

Feng L, Xu J and Kang SC (2016) Chemical composition of microbe-derived dissolved organic matter in cryoconite in Tibetan Plateau glaciers: insights from Fourier transform ion cyclotron resonance mass spectrometry analysis. *Environmental Science& Technology* **50**(24), 13215–13223. doi: 10.1021/acs.est.6b03971

Ficken KJ, Li B and Swain DL (2000) An *n*-alkane proxy for the sedimentary input of submerged/floating freshwater aquatic macrophytes. *Organic Geochemistry* **31**, 745–749. doi: 10.1016/S0146-6380(00)00081-4

Foreman CM, Sattler B and Mikucki JA (2007) Metabolic activity and diversity of cryoconites in the Taylor Valley, Antarctica. *Journal of Geophysical Research: Biogeosciences* **112**(G4), G04S32. doi: 10.1029/2006JG000358

Gelpi E, Oró J and Schneider HJ (1968) Olefins of high molecular weight in two microscopic algae. *Science* **161**(3842), 700–702. doi: 10.1126/science.161.3842.700

Gelpi E, Schneider H and Mann J (1970) Hydrocarbons of geochemical significance in microscopic algae. *Phytochemistry* **9**(3), 603–612. doi: 10.1016/S0031-9422(00)85700-3

Grimalt J and Albaigés J (1987) Sources and occurrence of C_{12}–C_{22} *n*-alkane distributions with even carbon-number preference in sedimentary environments. *Geochimica et Cosmochimica Acta* **51**, 1379–1384. doi: 10.1016/0016-7037(87)90322-X

Grimalt JO and Albaigés J (1990) Characterization of the depositional environments of the Ebro Delta (western Mediterranean) by the study of sedimentary lipid markers. *Marine Geology* **95**, 207–224. doi: 10.1016/0025-3227(90)90117-3

Han J and Calvin M (1969) Hydrocarbon distribution of algae and bacteria, and microbiological activity in sediments. *Proceedings of the National Academy of Sciences of the United States of America* **64**(2), 436–443. doi: 10.1073/pnas.64.2.436

Hockun K, Mollenhauer G and Ho SL (2016) Using distributions and stable isotopes of *n*-alkanes to disentangle organic matter contributions to sediments of Laguna Potrok Aike, Argentina. *Organic Geochemistry* **102**, 110–119. doi: 10.1016/j.orggeochem.2016.10.001

Hood E, Fellman J and Spencer RGM (2009) Glaciers as a source of ancient and labile organic matter to the marine environment. *Nature* **462**(24/31), 1044–1048. doi: 10.1038/nature08580

Hou JZ, D'Andrea WJ and MacDonald D (2007) Hydrogen isotopic variability in leaf waxes among terrestrial and aquatic plants around Blood Pond, Massachusetts (USA). *Organic Geochemistry* **38**, 977–984. doi: 10.1016/j.orggeochem.2006.12.009

Jaffé R, Mead R and Hernandez ME (2001) Origin and transport of sedimentary organic matter in two subtropical estuaries: a comparative, biomarker-based study. *Organic Geochemistry* **32**, 507–526. doi: 10.1016/s0146-6380(00)00192-3

Langford HJ, Irvine-Fynn TDL and Edwards A (2014) A spatial investigation of the environmental controls over cryoconite aggregation on Longyearbreen Glacier, Svalbard. *Biogeosciences (Online)* **11**, 5365–5380. doi: 10.5194/bg-11-5365-2014

Li L and Garzione CN (2017) Spatial distribution and controlling factors of stable isotopes in meteoric waters on the Tibetan Plateau: implications for paleoelevation reconstruction. *Earth and Planetary Science Letters* **460**, 302–314. doi: 10.1016/j.epsl.2016.11.046

Li L, Li QY and Tian J (2013) Low latitude hydro-climatic changes during the Plio-Pleistocene: evidence from high resolution alkane records in the southern South China Sea. *Quaternary Science Reviews* **78**, 209–224. doi: 10.1016/j.quascirev.2013.08.007

Li QL, Wang NL and Wu XB (2009) Compositional characteristics of *n*-alkanes of the glaciers over the Tibetan Plateau and their environmental and climatic significances. *Science in China Series D: Earth Sciences* **52**(11), 1803–1812. doi: 10.1007/s11430-009-0168-y

Li QL, Wang NL and Barbante C (2019) Biomass burning source identification through molecular markers in cryoconites over the Tibetan Plateau. *Environmental Pollution* **244**, 209–217. doi: 10.1016/j.envpol.2018.10.037

Liu YQ, Yao TD and Jiao NZ (2009) Bacterial diversity in the snow over Tibetan Plateau glaciers. *Extremophiles* **13**(3), 411–423. doi: 10.1007/s00792-009-0227-5

Luo P, Peng PA and Gleixner G (2011) Empirical relationship between leaf wax *n*-alkane δD and altitude in the Wuyi, Shennongjia and Tianshan Mountains, China: implications for paleoaltimetry. *Earth and Planetary Science Letters* **301**(1–2), 285–296. doi: 10.1016/j.epsl.2010.11.012

Matsumoto GI, Akiyama M and Watanuki K (1990) Unusual distributions of long-chain *n*-alkanes and *n*-alkenes in Antarctic soil. *Organic Geochemistry* **15**(4), 403–412. doi: 10.1016/0146-6380(90)90167-X

Meyers PA (2003) Applications of organic geochemistry to paleolimnological reconstructions: a summary of examples from the Laurentian Great Lakes. *Organic Geochemistry* **34**(2), 261–289. doi: 10.1016/S0146-6380(02)00168-7

Musilova M, Tranter M and Wadham J (2017) Microbially driven export of labile organic carbon from the Greenland ice sheet. *Nature Geoscience* **10**, 360–365. doi: 10.1038/ngeo2920

Patterson GW (1967) The effect of culture conditions on the hydrocarbon content of *Chlorella vulgaris*. *Journal of Phycology* **3**(1), 22–23. doi: 10.1111/j.1529-8817.1967.tb04623.x

Pautler BG, Dubnick A and Sharp MJ (2013) Comparison of cryoconite organic matter composition from Arctic and Antarctic glaciers at the molecular level. *Geochimica et Cosmochimica Acta* **104**, 1–18. doi: 10.1016/j.gca.2012.11.029

Pu Y, Wang CF and Meyers PA (2017) Origins of biomarker aliphatic hydrocarbons in sediments of alpine Lake Ximencuo, China. *Palaeogeography Palaeoclimatology Palaeoecology* **475**, 106–114. doi: 10.1016/j.palaeo.2017.03.011

Pu Y, Cao JC and Jia JH (2018) Unusual hydrocarbon waxes detected in *Salix oritrepha* leaf from Nianbaoyeze Mountains, eastern Qinghai-Tibetan Plateau. *Journal of Mountain Science* **15**(11), 2445–2452. doi: 10.1007/s11629-017-4646-y

Rozwalak P, Podkowa P and Buda J (2022) Cryoconite – from minerals and organic matter to bioengineered sediments on glacier's surfaces. *Science of the Total Environment* **807**(2), 150874. doi: 10.1016/j.scitotenv.2021.150874

Sachse D, Radke J and Gleixner G (2006) δD values of individual *n*-alkanes from terrestrial plants along a climatic gradient – implications for the sedimentary biomarker record. *Organic Geochemistry* **37**(4), 469–483. doi: 10.1016/j.orggeochem.2005.12.003

Sachse D, Billault I and Bowen GJ (2012) Molecular paleohydrology: interpreting the hydrogen-isotopic composition of lipid biomarkers from photosynthesizing organisms. *Annual Review of Earth and Planetary Sciences* **40**, 221–249. doi: 10.1146/annurev-earth-042711-105535

Sankelo P, Kawamura K and Seki O (2013) *n*-Alkanes in fresh snow in Hokkaido, Japan: implications for ice core studies. *Arctic Antarctic and Alpine Research* **45**(1), 119–131. doi: 10.1657/1938-4246-45.1.119

Schefuβ E, Schouten S and Schneider RR (2005) Climatic controls on central African hydrology during the past 20,000 years. *Nature* **437**(7061), 1003–1006. doi: 10.1038/nature03945

Schwark L, Zink K and Lechterbeck J (2002) Reconstruction of postglacial to early Holocene vegetation history in terrestrial Central Europe via cuticular lipid biomarkers and pollen records from lake sediments. *Geology* **30**, 463–466. doi: 10.1130/0091-7613(2002)0302.0.CO;2

Sikes EL, Uhle ME and Nodder SD (1993) Sources of organic matter in a coastal marine environment: evidence from *n*-alkanes and their $\delta^{13}C$ distributions in the Hauraki Gulf, New Zeal. *Phytochemistry* **34**(2), 381–387. doi: 10.1016/j.marchem.2008.12.003

Singer GA, Fasching C and Wilhelm L (2012) Biogeochemically diverse organic matter in Alpine glaciers and its downstream fate. *Nature Geoscience* **5**, 710–714. doi: 10.1038/ngeo1581

Smith HJ, Foster RA and McKnight DM (2017) Microbial formation of labile organic carbon in Antarctic glacial environments. *Nature Geoscience* **10**, 356–359. doi: 10.1038/nego2925

Snedaker SC, Glynn PW and Rumbold DG (1995) Distribution of *n*-alkanes in marine samples from southeast Florida. *Marine Pollution Bulletin* **30**(1), 83–89. doi: 10.1016/j.marchem.2017.08.002

Stibal M, Šabacká M and Žárský J (2012) Biological processes on glacier and ice sheet surfaces. *Nature Geoscience* **5**, 771–774. doi: 10.1038/ngeo1611

Takeuchi N (2002) Optical characteristics of cryoconite (surface dust) on glaciers: the relationship between light absorbency and the property of organic matter contained in the cryoconite. *Annals of Glaciology* **34**, 409–414. doi: 10.3189/172756402781817743

Takeuchi N and Li ZQ (2008) Characteristics of surface dust on Ürümqi glacier No. 1 in the Tien Shan Mountains, China. *Arctic Antarctic and Alpine Research* **40**(4), 744–750. doi: 10.1657/1523-0430(07-094)[TAKEUCHI]2.0.CO;2

Takeuchi N, Kohshima S and Seko K (2001) Structure, formation, and darkening process of albedo reducing material (cryoconite) on a Himalayan glacier: a granular algal mat growing on the glacier. *Arctic Antarctic and Alpine Research* **76727**(33), 115–122. doi: 10.1080/15230430.2001.12003413

Takeuchi N, Nagatsuka N and Uetake J (2014) Spatial variations in impurities (cryoconite) on glaciers in northwest Greenland. *Bulletin of Glaciological Research* **32**, 85–94. doi: 10.5331/bgr.32.85

Takeuchi N, Sakaki R and Uetake J (2018) Temporal variations of cryoconite holes and cryoconite coverage on the ablation ice surface of Qaanaaq Glacier in northwest Greenland. *Annals of Glaciology* **59**(77), 1–10. doi: 10.1017/aog.2018.19

Tedesco M, Doherty S and Fettweis X (2016) The darkening of the Greenland ice sheet: trends, drivers, and projections (1981–2100). *The Cryosphere* **10**, 477–496. doi: 10.5194/tc-10-477-2016

Wiltshire C, Waine TW and Grabowski RC (2023) Assessing *n*-alkane and neutral lipid biomarkers as tracers for land-use specific sediment sources. *Geoderma* **433**, 116445. doi: 10.1016/j.pocean.2021.102687

Xia ZH, Xu BQ and Mügler I (2008) Hydrogen isotope ratios of terrigenous *n*-alkanes in lacustrine surface sediment of the Tibetan Plateau record the precipitation signal. *Geochemical Journal* **42**, 331–338. doi: 10.2343/geochemj.42.331

Xie SC, Yao TD and Kang SC (2000) Geochemical analysis of a Himalayan snowpit profile: implication for atmospheric pollution and climate. *Organic Geochemistry* **31**, 15–23. doi: 10.1016/S0146-6380(99)00133-3

Xie SC, Nott CJ and Avsejs LA (2004) Molecular and isotopic stratigraphy in an ombrotrophic mire for paleoclimate reconstruction. *Geochimica et Cosmochimica Acta* **68**(13), 2849–2862. doi: 10.1016/j.gca.2003.08.025

Xu YP, Simpson AJ and Eyles N (2010) Sources and molecular composition of cryoconite organic matter from the Athabasca Glacier, Canadian Rocky Mountains. *Organic Geochemistry* **41**, 177–186. doi: 10.1016/j.orggeochem.2009.10.010

Yamada K and Ishiwatari R (1999) Carbon isotopic compositions of long-chain *n*-alkanes in the Japan Sea sediments: implication for paleoenvironmental changes over the past 85 kyr. *Organic Geochemistry* **30**(5), 367–377. doi: 10.1016/s0146-6380(99)00012-1

Yamamoto S, Kawamura K and Seki O (2011) Long-range atmospheric transport of terrestrial biomarkers by the Asian winter monsoon: evidence from fresh snow from Sapporo, northern Japan. *Atmospheric Environment* **45**(21), 3553–3560. doi: 10.1016/j.atmosenv.2011.03.071

Zhang YD, Su YL and Liu ZW (2015) Long-chain *n*-alkenes in recent sediment of Lake Lugu (SW China) and their ecological implications. *Limnologica* **52**, 30–40. doi: 10.1016/j.limno.2015.02.004

Zhang YD, Fu H and Yu JL (2023) Geochemical characteristics of *n*-alkanes in sediments from oligotrophic and eutrophic phases of five lakes and potential use as paleoenvironmental proxies. *Catena* **220**, 106682. doi: 10.1016/j.catena.2022.106682

Zhou L, Zhou YQ and Hu Y (2019) Microbial production and consumption of dissolved organic matter in glacial ecosystems on the Tibetan Plateau. *Water Research* **160**, 18–28. doi: 10.1016/j.watres.2019.05.048